

Antibody Screening Results for Anti-Nucleocapsid Antibodies Towards the Development of a SARS-CoV-2 Nucleocapsid Protein Antigen Detecting Lateral Flow Assay

David M. Cate¹, Helen V. Hsieh², Veronika A. Glukhova¹, Joshua D. Bishop¹, H. Gleda Hermansky², Brianda Barrios-Lopez², Ben D. Grant¹, Caitlin E. Anderson¹, Ethan Spencer¹, Samantha Kuhn¹, Ryan Gallagher¹, Rafael Rivera¹, Crissa Bennett², Sam A. Byrnes¹, John T. Connelly¹, Puneet K. Dewan¹, David S. Boyle³, Bernhard H. Weigl¹, Kevin P. Nichols^{1*}

1 - Global Health Labs, 14360 SE Eastgate Way, Bellevue, WA 98007

2 - Intellectual Ventures Laboratory, 14360 SE Eastgate Way, Bellevue, WA 98007

3 - PATH, 2201 Westlake Ave, Seattle, WA 98121

* Corresponding Author: Kevin Nichols – kevin.nichols@ghlabs.org

Abstract

The global COVID-19 pandemic has created an urgent demand for accurate rapid point of care diagnostic tests. Antigen-based assays are suitably inexpensive and can be rapidly mass-produced, but sufficiently accurate performance requires highly optimized antibodies and assay conditions. An automated liquid handling system, customized to handle lateral flow immunoassay (LFA) arrays, was used for high-throughput antibody screening of anti-nucleocapsid antibodies that will perform optimally on an LFA. Six hundred seventy-three anti-nucleocapsid antibody pairs were tested as both capture and detection reagents with the goal of finding those pairs that have the greatest affinity for unique epitopes of the nucleocapsid protein of SARS-CoV-2 while also performing optimally in an LFA format. In contrast to traditional antibody screening methods (e.g. ELISA, bio-layer interferometry), the methods described here integrate real-time LFA reaction kinetics and binding directly on nitrocellulose. We have identified several candidate antibody pairs that are suitable for further development of an LFA for SARS-CoV-2.

Introduction

The emergence of the severe acute respiratory syndrome coronavirus 2 (SARS-CoV-2) has led to a global pandemic of COVID-19, infecting more than fifteen million people worldwide in less than 8 months, and killing over 600,000 persons as of late July, 2020.^{1,2} Strategies to suppress transmission of SARS-CoV-2, the virus that causes COVID-19, have been constrained by limitations in the availability of tests that can detect viral infection early. The predominant test format used to detect SARS-CoV-2 is reverse transcriptase polymerase chain reaction (RT-PCR), conducted most commonly on specimens collected from the nasopharynx or oropharynx of symptomatic or exposed individuals. Demand for RT-PCR testing for SARS-CoV-2 has in most places exceeded available supply.

Diagnostic testing is central to detecting the virus in persons presenting with and without COVID-19 symptoms, or those identified as contacts exposed to COVID-19 cases, to guide community interventions that are predicted to contain ongoing transmission. The pandemic has resulted in unprecedented demand on the RT-PCR testing capacity of all countries. Demand for testing has been coupled with a global shortage of commercial kits, reagents, consumables, disruptions in the global transport networks, and exacerbated by international competition for testing resources. Accordingly, even many high-income countries have inadequate RT-PCR testing capacity to effectively suppress ongoing transmission, and most low and middle-income countries (LMICs) are unlikely to be able to establish even minimally needed RT-PCR capacity in the immediate future.

Direct antigen-based tests for SARS-CoV-2 offer an attractive alternative solution to testing needs and possibly the only viable solution for most LMICs. Antigen tests, which detect the presence of viral proteins, can be directly

conducted on biological samples, such as tissue swabbed from the anterior nasal cavity, oropharynx, or even directly on saliva. Such antigen tests already exist for influenza, strep throat, and other infectious diseases. LFA antigen tests in particular already have extremely high production capacities in the billions of units/year, are relatively inexpensive and easy to use, return results in minutes, and crucially, like RT-PCR and unlike serological tests, can reveal an active infection.

The use case for a low-cost, highly accessible SARS-CoV-2 assay is strong even if the assay were to be less sensitive than current RT-PCR testing. Modeling shows that decentralized, point-of-care testing with rapid return of results would have substantially greater potential impact on transmission than the absolute limit of detection of the assay.³ These models build on the important observation that infectious viral particles have not been recovered below around 100 copies/mL.^{4,5}

Rapid antigen tests are beginning to enter the commercial market. Thus far, however, few antigen tests for SARS-CoV-2 have received authorization from regulatory authorities worldwide. As of July 19th, 2020, two such products have received emergency use authorization (EUA) from the US Food and Drug Administration.^{6,7}

These FDA EUA authorized assays require instrumentation and are not available at low cost or outside health care settings. A concerted effort is underway to catalyze development of antigen-based rapid diagnostic tests that require no or minimal instrumentation, and to prepare manufacturing capability to meet the needs of the larger global market.⁸ The required performance characteristics of a SARS-CoV-2 antigen detection assay have not yet been published by the World Health Organization or other entities, but the FIND-UNITAID expression of interest proposes a minimum clinical sensitivity of 80%, and clinical specificity of 97% (compared to RT-PCR), to allow for large scale testing of moderate-risk populations.

A key step in the development of an LFA is the selection of the best antibodies. Our group has pioneered a high-throughput robotic antibody screening process directly on nitrocellulose.⁹ This method allows us to rapidly screen hundreds of combinations of antibodies far more quickly than is typical of early-stage LFA development while simultaneously utilizing nitrocellulose-specific reaction kinetics and flow rates that are difficult-to-impossible to mimic in other traditional multiplexed systems (e.g. ELISA, biolayer interferometry). Chemical gradients, residence times, binding orientations, affinity rates, drying and subsequent rehydration of reagents, and spatial distributions of antibodies are different in LFAs than in other immunoassays, and therefore, the best antibodies for LFAs may be different than for the best antibodies for ELISA, for example.

In this paper we describe the results of an extensive antibody screening effort that utilized our high-throughput robotic antibody screening platform⁹ to screen through 673 combinations of antibody pairs that target the SARS-CoV-2 nucleocapsid protein.

Materials and Methods

Reagents and materials

The following LFA reagents were purchased: TritonX-100, Tween-20, 10X PBS, sucrose, and IGEPAL (CA-630) from Sigma Aldrich (St. Louis, MO, USA); Surfactant-10G from Fitzgerald Industries (Acton, MA, USA); 20× Borate, pH 8.5 and 10× PBST from Thermo Fisher Scientific (Waltham, MA, USA); PBS tablets from VWR (Radnor, PA, USA); BSA from Seracare Life Sciences (Milford, MA, USA).

SARS-CoV-2 nucleocapsid antigens were purchased from Acro Biosystems (Cat. No. NUN-C5227), Creative Diagnostics (Cat. No. DAGC094), Genemedi (Cat. No. GMP-V-2019nCoV-N002), Genscript (Cat. No. Z03480-1), MyBiosource (Cat. No. MBS7135899), Sino Biological (Cat. No. 40588-V088), and The Native Antigen Co. (Cat. No. REC31812-100). A list of anti-nucleocapsid antibodies screened in this work are provided in Table 2si (supp. info).

The following LFA materials were used for antibody screening: backed nitrocellulose (20 mm wide, CN95, Sartorius Lab Instruments GmbH & Co. KG, Otto-Brenner-Straße 20, Göttingen, Germany), conjugate pad (10 mm wide, No. 6613, Ahlstrom-Munksjö, Oyj, Finland), sample pad (18 mm wide, Cat. No. 1281, Ahlstrom-Munksjö), wicking pad (14 mm wide, Cat. No. 440, Ahlstrom-Munksjö), cover tape (13 mm wide, Cat. No. 300H2, 3M, St. Paul, MN, USA) and backing card (50 mm wide, Cat. No. KN2211, Kenosha, Schweitzerlaan, The Netherlands).

All primers and probes, purified 2019-nCoV_N RNA, and Hs_RPP30 human RNA were purchased from IDT (Coralville, IA, USA). The Research Use Only (RUO) QIAamp Viral Mini Kit for RNA extraction was purchased from Qiagen (Hilden, Germany). The qScript XLT 1-Step RT-qPCR ToughMix was purchased from QuantaBio (Beverly, MA, USA). Molecular biology grade water was purchased from Fisher Scientific (Waltham, MA, USA).

A total of nine de-identified samples were purchased from Medix (Lombard, IL, USA). These samples included six SARS-CoV-2 positives and three negatives. All samples were discarded and de-identified and therefore did not require IRB approval for use.

RT-qPCR for detection of COVID-19 and quantification of SARS-CoV-2 viral load

The COVID-19 status of clinical samples used in this work was determined in-house using a multiplex RT-qPCR for the N1, N2, and RP targets.¹⁰ Briefly, 70 or 140 µL of sample were purified using the QIAamp Viral Mini Kit according to the manufacturer's protocol¹¹ and purified RNA was eluted in either 70 or 140 µL based on CDC recommendations.¹² The multiplexed reaction was performed using the qScript master mix from QuantaBio with N1 and RP primers and probe concentrations of 500 nM and 125 nM (final) and N2 primers and probe concentrations of 2000 nM and 500 nM (final). The probes used were N1-FAM, N2-AlexaFluor594, and RP-Cy5. For each reaction, 5 µL of sample was added to 15 µL of amplification mix. Samples were classified as positive if both N1 and N2 targets were detected with Ct values below 40 cycles.¹³ Viral load was determined using a standard curve for the N1 target generated from purified 2019-nCoV_N RNA. The purified SARS-CoV-2 RNA was quantified in-house using the BioRad QX200 Digital Droplet PCR System.

Antigen selection using Octet

Antibody-antigen interactions were evaluated with an Octet® RED96 biolayer interferometry instrument (Molecular Devices, Sartorius AG, Göttingen, Germany). All measurements were performed in 96-well microplates (Greiner Bio-one, Frickenhausen, Germany) at ambient temperature. Antibodies were loaded at 25 nM in 1× Kinetics Buffer for 120 seconds and captured using AMC tips for mouse antibodies, AHC tips for humanized recombinant antibodies, and Protein A tips for rabbit antibodies. Materials for the Octet were purchased from Molecular Devices. New sensors were used for every reaction and no tip regeneration was performed.

Typical immobilization levels were 1 ± 0.2 nm for monoclonal antibodies, and 2 nm for rabbit polyclonal antibodies. Following the load step, all sensors were equilibrated to baseline for 120 seconds in 1× Kinetics Buffer. Association step was performed for 300 seconds with antigen at 100 nM quantity, followed by 300 second dissociation into 1× Kinetics buffer.

Antibody/antigen evaluation by SDS-PAGE

Antigens were evaluated for purity and size using SDS-PAGE. Concentration was measured for all proteins using BCA assay (Thermo Pierce cat. 23225). Samples were premixed NuPAGE™ LDS Sample Buffer (4×) (Thermo Pierce cat. NP0007) and heated at 70°C for 10 minutes. Gels with a 4-12% Bis-Tris gradient were used to achieve separation. Coomassie Imperial™ Protein Stain (Thermo Pierce cat. 24615) was used to visualize bands. Novex Sharp Pre-stained protein standard (Thermo Fisher scientific) was used as a molecular weight marker.

Latex bead conjugation

For both test and control line detection conjugates, 400 nm carboxylic blue latex beads (Cat. No. CAB400NM, Magsphere, Pasadena CA, USA) were washed three times with 0.1M MES buffer, pH 6. Then, latex beads were activated using EDC/NHS coupling reagents at 0.15 and 10 mg/mL respectively for 30 minutes. Afterwards, the blue latex particles were conjugated in 1× PBS, pH 7.2 to various anti-nucleocapsid antibodies at a w/w ratio of 20:1 and 10:1 (bead: antibody) for test and control line antibodies, respectively, for three hours. Finally, latex conjugates were quenched using 0.1M ethanolamine before being washed and blocked with 6% (w/v) casein, final concentration 1.2%, overnight. The latex conjugates were stored in buffer containing 50mM borate and 1% casein, pH 8.5. The latex conjugates were quantified using the spectrophotometer by measuring absorbance at 660 nm and comparing to absorbance of unconjugated beads.

LFA reagent deposition

Capture antibodies at 1 mg/mL in 1× PBS, pH 7.4 and 2.5% (w/v) sucrose were striped (ZX1010, BioDot, Irvine, CA, USA) on nitrocellulose CN95 and dried at 25°C for 30 min. The control line was striped at 0.75 mg/mL Donkey anti-Chicken IgY (Cat. No. 703-005-155, Jackson ImmunoResearch, West Grove, PA, USA). For antibody screening, the nitrocellulose was unblocked. The test and control lines were located at 8 mm and 13 mm from the upstream edge of the nitrocellulose membrane.

The conjugate pad was dip-coated with two blocking solutions. First, 6613 conjugate pads were soaked in a 0.05% (w/v) Tween-20 in diH₂O solution for 15–20 seconds and dried at 40°C for 60 min. Pads were again soaked in 50mM borate, pH 8.5; 0.25% (w/v) Triton X-100; 1% (w/v) Surfactant-10G; 1% (w/v) sucrose; and 6% (w/v) casein for another 15–20 seconds. The conjugate pad was dried for 60 min at 40°C before assembly.

LFA Assembly

Card assembly was performed on a clamshell laminator (Matrix 2210, Kinematic Automation, Sonora CA, USA). Pads were placed on the backing card in the following order: nitrocellulose, cover tape, conjugate pad, sample pad, wicking pad. Individual strips (3.3 mm wide) were cut with a Matrix 2360 sheet cutter (Kinematic Automation) and assembled in cassettes (proprietary design) using an assembly roller (YK725, Kinbio Tech Co., Shanghai, China).

Hamilton screening procedure

Antibody pairs were screened on an integrated robotic system⁹ we have previously used to test antibody performance directly on nitrocellulose. In this system, the Hamilton STAR automated liquid handling robot (Hamilton Company, Reno, NV, USA), camera (IDS UI-1460SE-C-H detector with a Tamron M118FM16 lens) custom LFA holders, and custom control software developed in-house were combined to allow rapid screening of antibody pairs directly in LFA format. The robot used 8-channel pipetting for parallel application to LFAs and the camera for imaging. The custom LFA framework held a maximum of 96 LFA cassettes per robot run. The custom control software applied 1 µL of latex bead conjugate mix (0.15% anti-nucleocapsid -latex bead, 0.1% or 0.05% Chicken IgY latex bead in 50mM borate pH 8.5) to the conjugate pad in the LFA. After a 10-minute delay to let the conjugate mix dry, 75 µL of sample, nucleocapsid protein or buffer (2.5% BSA in PBST or 2.5% BSA and 1% IGEPAL in 1× PBS) was added to the sample pad. Images were acquired 20 minutes after sample addition. Four technical replicates were run for each antibody pair per sample type.

Screening recombinant antigens on LFAs

We conducted four rounds of testing using recombinant NP as the antigen target. The first, with the best-available available NP antigen, at 50 ng/mL. The second, with a subsequently determined preferable antigen, at 50 ng/mL. A third round, under the same conditions but with data-driven down-selection of antibody pairs, and the fourth, with 25 ng/mL. A complete list of all pairs screened from all rounds is in Table 1si (supp. info).

Screening clinical samples on LFAs

In-house RT-qPCR was performed on banked nasopharyngeal clinical samples to confirm infection status prior to LFA testing (Table 1). When testing clinical samples, test and control line conjugates were hand spotted prior to sample application. The test line conjugate was diluted to a final concentration of 0.10% and control line Chicken IgY conjugate to 0.15% in 50 mM Borate, pH 8.5. First, 1 μ L of conjugate mixture was pipetted onto the conjugate pad and allowed to dry at ambient temp for 10 minutes prior to application of the sample. All samples were diluted 1:25 in sample buffer containing 2.5% BSA and 1% IGEAL in 1x PBS. Samples were incubated on ice for 30 minutes prior to use. Second, 75 μ L of each sample diluted in sample buffer was added to the conjugate pad and run at ambient conditions inside a biosafety cabinet for 20 minutes prior to being read in an LFA reader.

Table 1 | Banked samples were used to compare performance of select anti-nucleocapsid antibody pairs in LFAs. In total, six RT-qPCR-confirmed SARS-CoV-2 positives, three SARS-CoV-2 negatives, and two potential coronavirus cross-reactive samples were screened.

Patient ID / Cat. No.	Clinical SARS-CoV-2 NAAT Results (pos v. neg)	SARS-CoV-2 Viral Load (c/uL, using purified RNA, N1 gene)	1:25 dilution, viral load (c/uL)	Human RNA Load (c/uL, using purified RNA, RP gene)	Vendor
4175017	+	3.5E+08	1.4E+07	9.2E+00	Medix Biochemica
4187771	+	2.2E+08	8.8E+06	1.4E+00	Medix Biochemica
4186565	+	1.5E+08	6.1E+06	2.1E+00	Medix Biochemica
4184163	+	7.3E+07	2.9E+06	-	Medix Biochemica
4182846	+	1.9E+06	7.6E+04	1.2E+04	Medix Biochemica
4183188	+	8.4E+05	3.4E+04	5.7E+01	Medix Biochemica
4177740	-	-	-	-	Medix Biochemica
4182799	-	-	-	1.6E+05	Medix Biochemica
4184232	-	-	-	6.1E+03	Medix Biochemica
HCoV-NL63 coronavirus	n/a	n/a	n/a	n/a	Abcam
HCoV-229E lysate VR740™	n/a	n/a	n/a	n/a	ATCC

Data analysis

Image analysis for the integrated robotic system was performed with a custom Python-based tool developed in-house.⁹ This tool identified the test and control lines, measured nitrocellulose background intensity, and reported signal from the height of the line peak. Faulty LFAs were identified by low control line signal or poor shape and removed as outliers, however outlier removal was rare, occurring in fewer than 2% of all LFAs tested. The results were analyzed by calculating the average response for antigen positive samples, antigen negative samples, and the ratio and difference between these two signals.

Antibody pair rankings were determined by quantifying signal intensity divided by background noise (non-specific binding) and signal intensity subtracted by background noise-. Both metrics were used to increase the requirements of the best pairs to have both high positive control signal and low negative control signal. Four technical replicates were measured for all LFAs in the robotic screen portion of this work.

For benchtop analysis of LFAs, test and control line intensities were quantified using a LED-based LFA reader (Axxin, Fairfield, Australia).

Results and Discussion

Biolayer interferometry was performed on recombinant nucleocapsid proteins (NPs), for the purpose of selecting the most “native-like” analyte for LFA antibody screening. Initially, we used the estimated R_{\max} of five different NPs to quantify binding affinity against a random selection of 21 anti-nucleocapsid antibodies from seven different vendors (Rockland, Novus Biologicals, Sino Biological, Creative Diagnostics, Bioss, Fitzgerald, and MyBiosource). The metric R_{\max} was calculated based on theoretically saturating 100% of the bound antibody (ligand) with the analyte (NP). In practice, analyte binding sites are not completely occupied, so the measured saturation value is typically less than R_{\max} . Moreover, because R_{\max} is proportional to analyte size, we were also able to detect aggregation or multimer formation in solution. In theory, the closer—and more predictable—measured values were to R_{\max} the more likely the antigen was to interact with antibodies as expected. The NP antigen from Genemedi was selected as the starting antigen for antibody screening because the average saturation value across 21 different anti-NP antibodies was closest to the theoretical R_{\max} of the antigen (data not provided).

Round 1 of antibody pair screening on LFAs consisted of a 11×11 grid of antibodies (121 unique pairs). For each pair, one antibody was striped on nitrocellulose as a test line (the “capture” antibody) and the other was coupled to latex nanoparticles using EDC/NHS chemistry (the “detector” antibody). The results of the first round are given in Figure 1(A). The positive control for round 1 was 50 ng/mL NP from Genemedi. The negative control was 2.5% BSA in PBST. The top five antibody pairs after round 1 for both S/N and S-N were index pairs 540, 567, 564, 604, and 603 (Table 2). As anticipated, self-pairs did not perform well compared to non-self-pairs because Genemedi’s nucleocapsid protein was monomeric and therefore likely to only contain a single copy of the sequence targeted by antibodies in the screen. Competition for the same epitope likely reduced the number of complete sandwich formation at the test line. Octet analysis also confirmed poor self-pair performance (data not shown). After completing round 1, 75 pairs were eliminated from further evaluation. To maintain a large antibody pair pool for subsequent rounds, any pair in the top 20 for S-N or S/N were re-screened in round 2, along with three new anti-NP antibodies.

The grid for round 2 was 11×11 (121 pairs); every antibody was evaluated as both capture and detectors. Results from round 2 are in Figure 1(B). The positive NP control was 50 ng/mL from Acro Biosystems. The negative control was 2.5% BSA in PBST. A new NP vendor was used for round 2 because we observed more consistent antibody binding (Octet measurement of binding saturation relative to R_{\max} , data not provided) against a random selection of anti-NP antibodies when compared head-to-head with the Genemedi NP antigen used in round 1. Additionally, the antigen from Acro Biosystems was expressed in HEK293T cells whereas Genemedi’s NP was *E. coli* produced; therefore, the mammalian cell expressed protein was most likely to display the biologically-relevant glycosylation patterns that viral proteins from infected human cells would express. Based on S/N and S-N metrics, the five best performing antibody pairs from round 2 were 33, 355, 653, 7, and 533 (Table 2). All five pairs from round 1 were in the top 60% of performers in round 2, and in total, 114 pairs were eliminated in round 2 from further examination.

Round 3 of screening contained seven pairs from round 2 and seven new anti-NP antibodies, again evaluated as both capture and detectors. By the third round, seven antibody pairs were producing strong signal intensity at the test line at 50 ng/mL, so another decision was made to reduce concentration of the Acro Biosystems NP antigen from 50 to 25 ng/mL to increase selectivity and emphasize the highest-performing pairs. The grid for round 3 was 12×12 (144 pairs). Results are displayed in Figure 1(C). The top five performers from round 3 by S/N and S-N were index pairs 533, 70, 50, 7, and 33 (Table 2). Three pairs (7, 533, and 33) were top-five performers from a previous round. Another 114 pairs were eliminated from further examination and 30 pairs were re-evaluated in round 4.

Antigen concentration for round 4 was decreased again from 25 to 10 ng/mL. The antibody pair grid size was 18 × 18 (324 pairs) to accommodate 12 new anti-NP antibodies. The top five performing pairs against the Acro Biosystems NP were 423, 33, 70, 422, and 403 (Table 2, Figure 1(D)). Pairs 33 and 70 were again repeated from earlier rounds, indicating that antibodies in these pairs had high affinity for the antigen from Acro Biosystems.

After concluding four rounds of screening, 673 unique anti-NP pairs had been screened with a combination of antigens from two different vendors (Genemedi and Acro Biosystems) and three different spike concentrations (50, 25, and 10 ng/mL), which was necessary because the average pair performance was reaching the non-linear peak of test line intensity. A complete list of all pairs screened are indexed in Table 1si (supp. info).

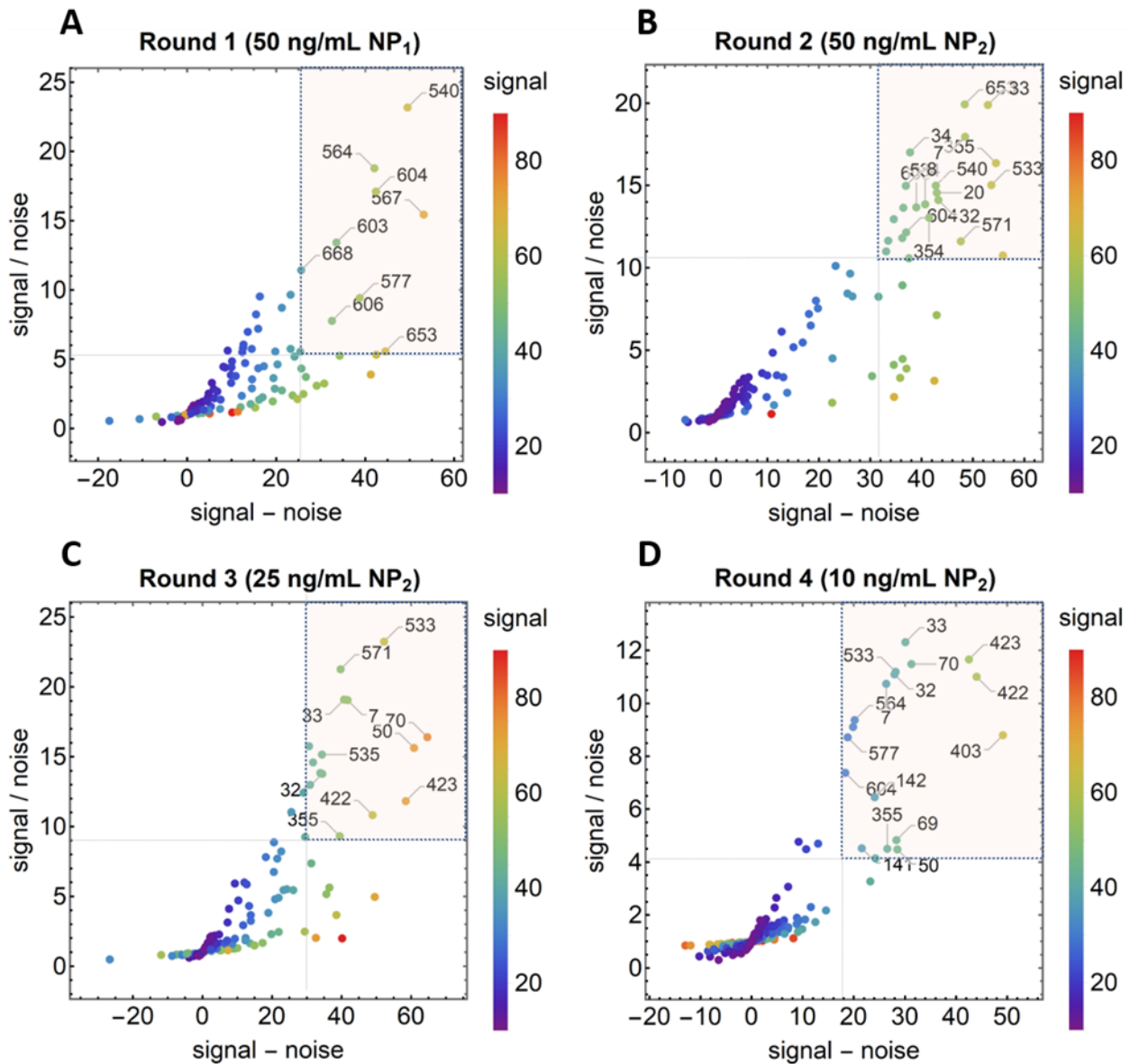


Figure 1 | A Performance of 673 individual antibody pairs in 4 rounds of screening as a function of signal / noise and signal - noise. Line intensities are shown as scatter plots for round 1 (**A**), round 2 (**B**), round 3 (**C**), and round 4 (**D**). Antibody pairs in the top 20 for both S/N and S-N are overlaid with a semi-transparent box and numbered by their index (full list in Table 1si). NP₁ antigen was sourced from GeneMedi and NP₂ antigen was sourced from Acro Biological.

Table 2 | Antibody pairs in the top 20 for both S/N and S-N are ranked according to the round in which they were tested. Pair 33 performed in the top 5 for rounds 2, 3, 4. Pairs 7 and 533 in top 5 for rounds 2, 3. Pair 70 in top 5 for rounds 3, 4. Table 1si (supp. info) contains a complete list of all pairs screened.

Index	Capture antibody	Detector antibody	Average rank			
			rd. 1	rd. 2	rd. 3	rd. 4
Top 5 performers (round 1)						
540	Sino Biological 40143-MM08	Creative Diagnostics DCABH-4693	1.5	9	-	-
567	Sino Biological 40143-MM08	Sino Biological 40143-R004	2.5	25	-	-
564	Sino Biological 40143-MM08	Sino Biological 40143-MM05	4	21.5	14	12
604	Sino Biological 40143-R001	Sino Biological 40143-MM08	4	17.5	25	15.5
603	Sino Biological 40143-R001	Sino Biological 40143-MM05	7.5	13.5	19	13
Top 5 performers (round 2)						
33	Bioss bsm-41411M	Sino Biological 40143-MM08	-	3	5.5	3
355	Fitzgerald 10-2856	Sino Biological 40143-MM08	-	3.5	14	14.5
653	Sino Biological 40143-R040	Sino Biological 40143-MM08	11.5	3.5	16.5	-
7	Bioss bsm-41411M	Creative Diagnostics CABT-CS037	-	4	5.5	8.5
533	Sino Biological 40143-MM08	Bioss bsm-41411M	-	4.5	2.5	6
Top 5 performers (round 3)						
533	Sino Biological 40143-MM08	Bioss bsm-41411M	-	4.5	2.5	6
70	Bioss bsm-41413M	Sino Biological 40143-MM08	-	-	3	3.5
50	Bioss bsm-41413M	Creative Diagnostics CABT-CS037	-	-	4.5	13
7	Bioss bsm-41411M	Creative Diagnostics CABT-CS037	-	4	5.5	8.5
33	Bioss bsm-41411M	Sino Biological 40143-MM08	-	3	5.5	3
Top 5 performers (round 4)						
423	Genemedi GMP-V- 2019nCoV-NAb001	Sino Biological 40143-MM08	-	-	8.5	2.5
33	Bioss bsm-41411M	Sino Biological 40143-MM08	-	3	5.5	3
70	Bioss bsm-41413M	Sino Biological 40143-MM08	-	-	3	3.5
422	Genemedi GMP-V- 2019nCoV-NAb001	Sino Biological 40143-MM05	-	-	11	4
403	Genemedi GMP-V- 2019nCoV-NAb00	Creative Diagnostics CABT-CS037	-	-	19	5.5

Another important feature of screening large numbers of antibody pairs in an LFA format is the ability to identify pairs that non-specifically bind at the test line. The unique interplay of flow dynamics and chemical kinetics across reagents and materials in an LFA means that screening data from non-LFA formats sometimes does not predict non-specific binding in an LFA format. We have found that screening data from the high-throughput robotic platform does predict non-specific binding in the LFA even when screened with different sample matrices, such as clinical negatives at multiple dilutions (Figure 2si). Additionally, several rounds of negative sample screening data can often be combined—even if positive samples are varied across rounds—if the negative samples are consistent across rounds, as was the case here. Combined negative sample data was used to remove pairs from contention when non-specific binding was greater than a self-defined threshold (e.g. a nominal specificity target), which was helpful because the number of pairs was large. This method reduced the likelihood that a high positive signal was primarily driven by non-specific binding and performing well artificially.

To demonstrate the difference between pairs identified as *high*, *moderate*, and *low*-performers, we selected 16 pairs with which to screen banked clinical SARS-CoV-2 positive, negative, and potentially cross-reactive samples. The two cross-reactive samples tested were confirmed positive for non-SARS-CoV-2 coronavirus (types 229E and NL63). No additional optimization of the LFA was performed beyond basic steps such as blocking the conjugate pad. Results from the clinical screen are shown in Figure 2. The top and bottom charts measure performance as a function of S-N and S/N, respectively. Signals were derived from three technical replicates on up to four positive clinical samples. Noise was pooled from three technical replicates across a blank sample and/or up to three negative clinical samples. Two additional positive clinical samples were tested but showed little-to-no response across all pairs and were excluded from the analysis. Finally, the S-N and S/N results corresponding to each positive sample were normalized by the logarithm of the viral load in each positive sample to allow for a more accurate performance comparison across test conditions.

The data showed that the best pairs (e.g. index pairs 567, 527) were at least 15-fold higher in S-N intensity, on average, across all positive samples when compared with LFA pairs identified in the screen as poor performers (e.g. index pairs 666, 517). Signal intensities varied for different clinical positives, as expected, however 2/6 samples (IDs 846 and 188, Table 1) were not visible on any LFA and were therefore excluded from analysis. A complete dataset is provided in Figure 1si (supp. info). After dilution, the viral load of these two samples was $3\text{--}7 \times 10^4$ (c/μL), indicating the LOD of these LFAs, without additional optimization is roughly 1×10^5 c/μL. A previous paper from our group reported the optimization of a half-strip LFA targeting SARS-CoV-2 viral NP.¹⁴ There was no visible non-specific binding or cross-reactivity to related coronavirus samples 229E and NL63 (Figure 1, supp. info), but additional screening of potential cross-reactivity should be performed on candidate pairs. The LFAs that performed the best against clinical positive, negative, and potentially reactive samples used antibody index pairs 567, 527, 564, and 111 (Table 3).

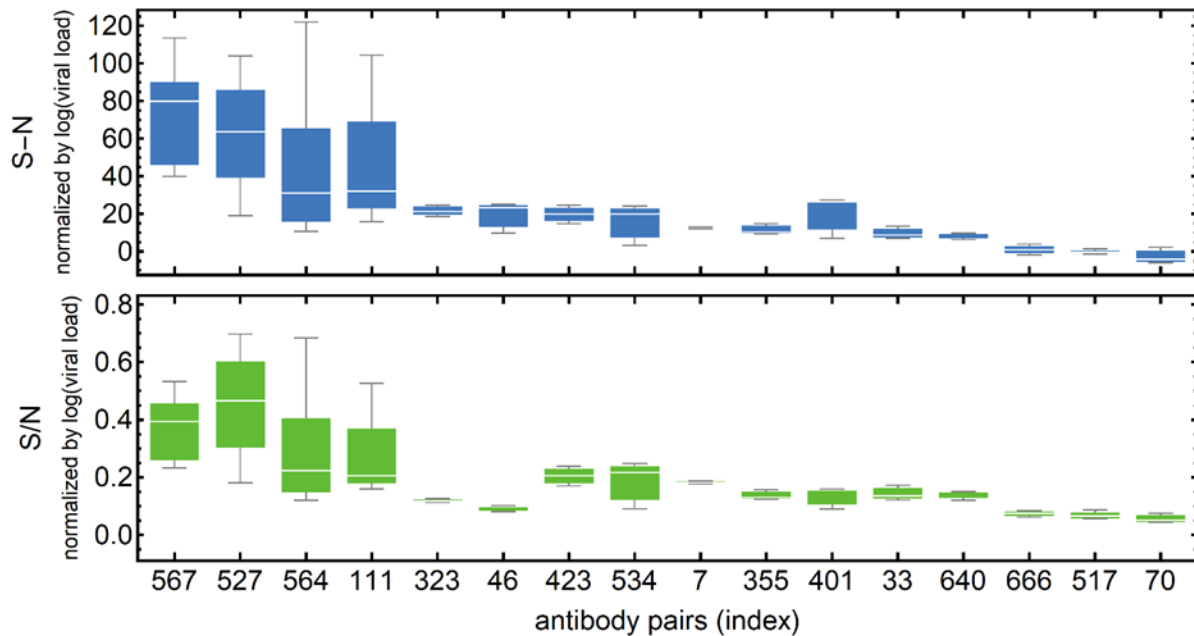


Figure 2 | Performance of 16 selected antibody pairs on clinical samples as a function of signal – noise (S-N) (TOP graph) and signal / noise (S/N) (BOTTOM graph).

Interestingly, pairs testing well in rounds 2–4 wherein NP from Acro Biosystems was the target did not perform as well as expected in the clinical screen. Table 3si in supp. info ranks pairs from the clinical screen as well as each pair’s ranking (avg. of S/N and S-N) in rounds 1–4. Index pairs 33, 70, 7, and 423, for example, were top-10 performers in one or more rounds, however in the clinical screening round, the average S-N intensity across all positive samples was 75-94% lower than the best performing pair (index pair 567). Specific antibodies (e.g. Bioss bsm-41411M) appeared to have higher affinity for the antigen from Acro Biosystems but performed below expectation when were included in pairs that were tested against banked clinical samples pairs contained this antibody underperformed expectations. The *E. coli* produced antigen from Genemedi appeared to best predict antibody pair performance against clinical samples, however additional investigation is warranted.

Table 3 | Antibody pairs selected to be screened against clinical samples are ranked according to average performance by S-N and S/N in the clinical screen. Table 3si (supp. info.) includes a full list of average rankings from all four high-throughput robotic platform screening rounds.

Index	Capture antibody	Detector antibody	Avg. Rank
567	Sino Biological 40143-MM08	Sino Biological 40143-R004	1
527	Sino Biological 40143-MM05	Sino Biological 40143-MM08	2
564	Sino Biological 40143-MM08	Sino Biological 40143-MM05	3
111	Creative Diagnostics CABT-CS037	Sino Biological 40143-R004	4.5
423	Genemedi GMP-V- 2019nCoV-NAb001	Sino Biological 40143-MM08	5.5
7	Bioss bsm-41411M	Creative Diagnostics CABT-CS037	7.5
534	Sino Biological 40143-MM08	Bioss bsm-41412M	7.5
323	Fitzgerald 10-2856	Bioss bsm-41411M	8
46	Bioss bsm-41413M	Bioss bsm-41411M	9.5
355	Fitzgerald 10-2856	Sino Biological 40143-MM08	9.5
640	Sino Biological 40143-R040	Creative Diagnostics CABT-CS037	10.5
33	Bioss bsm-41411M	Sino Biological 40143-MM08	11
401	Genemedi GMP-V- 2019nCoV-NAb001	Bioss bsm-41413M	11.5
517	Novus Bio NB100- 56683	Sino Biological 40143-MM05	14.5
666	Sino Biological 40588-T62	Novus Bio NB100-56683	14.5
70	Bioss bsm-41413M	Sino Biological 40143-MM08	16

Conclusions

Six hundred seventy-three antibody pairs were screened against SARS-CoV-2 nucleocapsid protein, and multiple candidates from several different commercially available sources were identified as promising candidates towards the development of lateral flow assays for the detection of SARS-CoV-2. Further work is required for the development of a point-of-care test for SARS-CoV-2, though the antibodies screened within this paper provide a necessary step towards its development. The antibody pairs that we identify as the top-ranking pairs should be interpreted as down-selected, though not necessarily precisely ordered list of the best potential candidates for developing an LFA. We suggest that multiple of the top pairs we identified be tested further by anyone attempting to develop an LFA using these data, as the precise interaction of all assay components, materials, and methods can affect which pair will perform optimally.

Acknowledgements

Funding provided by The Global Good Fund and Global Health Labs, a nonprofit organization created by Gates Ventures and the Gates Foundation to develop innovative solutions to address unmet needs in primary health care centers and the last mile.

References

- (1) Zhu, N.; Zhang, D.; Wang, W.; Li, X.; Yang, B.; Song, J.; Zhao, X.; Huang, B.; Shi, W.; Lu, R.; Niu, P.; Zhan, F.; Ma, X.; Wang, D.; Xu, W.; Wu, G.; Gao, G. F.; Tan, W. A Novel Coronavirus from Patients with Pneumonia in China, 2019. *N. Engl. J. Med.* **2020**, *382* (8), 727–733. <https://doi.org/10.1056/NEJMoa2001017>.
- (2) Coronavirus disease (COVID-19) Situation Report https://www.who.int/docs/default-source/coronaviruse/situation-reports/20200723-covid-19-sitrep-185.pdf?sfvrsn=9395b7bf_2 (accessed Jul 23, 2020).
- (3) Larremore, D. B.; Wilder, B.; Lester, E.; Shehata, S.; Burke, J. M.; Hay, J. A.; Tambe, M.; Mina, M. J.; Parker, R. Test Sensitivity Is Secondary to Frequency and Turnaround Time for COVID-19 Surveillance. *medRxiv* **2020**, 2020.06.22.20136309. <https://doi.org/10.1101/2020.06.22.20136309>.
- (4) He, X.; Lau, E. H. Y.; Wu, P.; Deng, X.; Wang, J.; Hao, X.; Lau, Y. C.; Wong, J. Y.; Guan, Y.; Tan, X.; Mo, X.; Chen, Y.; Liao, B.; Chen, W.; Hu, F.; Zhang, Q.; Zhong, M.; Wu, Y.; Zhao, L.; Zhang, F.; Cowling, B. J.; Li, F.; Leung, G. M. Temporal Dynamics in Viral Shedding and Transmissibility of COVID-19. *Nat. Med.* **2020**, *26* (5), 672–675. <https://doi.org/10.1038/s41591-020-0869-5>.
- (5) Alexandersen, S.; Chamings, A.; Bhatta, T. R. SARS-CoV-2 Genomic and Subgenomic RNAs in Diagnostic Samples Are Not an Indicator of Active Replication. *medRxiv* **2020**, 2020.06.01.20119750. <https://doi.org/10.1101/2020.06.01.20119750>.
- (6) Sofia SARS Antigen FIA <https://www.fda.gov/media/137885/download> (accessed Jul 23, 2020).
- (7) Veritor System For Rapid Detection of SARS-CoV-2 <https://www.fda.gov/media/139755/download> (accessed Jul 23, 2020).
- (8) Expression of interest - FIND <https://www.finddx.org/eoi-covid19-ag-rdt/> (accessed Jul 23, 2020).
- (9) Huynh, T.; Cate, D. M.; Nichols, K. P.; Weigl, B. H.; Anderson, C. E.; Gasperino, D. J.; Harston, S. P.; Hsieh, H. V.; Marzan, R.; Williford, J. R.; Oncina, C. I.; Glukhova, V. A. Integrated Robotic System for the Development Lateral Flow Assays. In *2019 IEEE Global Humanitarian Technology Conference, GHTC 2019*; Institute of Electrical and Electronics Engineers Inc., 2019. <https://doi.org/10.1109/GHTC46095.2019.9033066>.
- (10) Byrnes, S. A.; Gallagher, R.; Steadman, A.; Bennett, C.; Rivera, R.; Ortega, C.; Motley, S. T.; Jain, P.; Weigl, B. H.; Connelly, J. T. Multiplexed and Extraction-Free Amplification for Simplified SARS-CoV-2 RT-PCR Tests. *medRxiv* **2020**, 2020.05.21.20106195. <https://doi.org/10.1101/2020.05.21.20106195>.
- (11) QIAamp Viral RNA Mini Handbook - QIAGEN <https://www.qiagen.com/us/resources/resourcedetail?id=c80685c0-4103-49ea-aa72-8989420e3018&lang=en> (accessed Jul 23, 2020).
- (12) *CDC 2019–Novel Coronavirus (2019–NCoV) Real-Time RT-PCR Diagnostic Panel For Emergency Use Only Instructions for Use*.
- (13) Bustin, S. A.; Benes, V.; Garson, J. A.; Hellems, J.; Huggett, J.; Kubista, M.; Mueller, R.; Nolan, T.; Pfaffl, M. W.; Shipley, G. L.; Vandesompele, J.; Wittwer, C. T. The MIQE Guidelines: Minimum Information for Publication of Quantitative Real-Time PCR Experiments. *Clin. Chem.* **2009**, *55* (4), 611–622. <https://doi.org/10.1373/clinchem.2008.112797>.
- (14) Grant, B. D.; Anderson, C. E.; Williford, J. R.; Alonzo, L. F.; Glukhova, V. A.; Boyle, D. S.; Weigl, B. H.; Nichols, K. P. A SARS-CoV-2 Coronavirus Nucleocapsid Antigen-Detecting Half-Strip Lateral Flow Assay Towards the Development of Point of Care Tests Using Commercially Available Reagents. *Anal. Chem.* **2020**. <https://doi.org/10.1021/acs.analchem.0c01975>.